TOPICAL REVIEW — Terahertz physics

Research progress in terahertz quantum-cascade lasers and quantum-well photodetectors*

Zhi-Yong Tan(谭智勇)[1,2], Wen-Jian Wan(万文坚)[1], and Jun-Cheng Cao(曹俊诚)[1,2,†]

[1] *Key Laboratory of Terahertz Solid-State Technology, Shanghai Institute of Microsystem and Information Technology, Chinese Academy of Sciences, Shanghai* 200050, *China*

[2] *Center of Materials Science and Optoelectronics Engineering, University of Chinese Academy of Sciences, Beijing* 100049, *China*

(Received 4 May 2020; revised manuscript received 15 July 2020; accepted manuscript online 27 July 2020)

As semiconductor devices, the terahertz quantum-cascade laser is a coherent source based on intersubband transitions of unipolar carriers while the terahertz quantum-well photodetector is a kind of detector which matches the laser frequency. They are solid-state, electrically operated, and can be easily integrated with other components. This paper reviews the state of the art for the design, working performance, and future directions of the two devices. Their applications in photoelectric characterization and imaging are also discussed.

Keywords: terahertz, semiconductor device, photoelectric characterization, imaging system

PACS: 42.55.Px, 85.60.Bt, 42.30.−d, 95.85.Gn **DOI:** 10.1088/1674-1056/aba945

1. Introduction

Terahertz quantum-cascade lasers (QCLs)[1] and quantum-well detectors (QWPs)[2] are optoelectronic devices based on low dimensional compound semiconductor materials, which are very important sources and photodetectors in terahertz region. They have the characteristics of compact configuration, mature fabrication process, stable performance, and easy integration. They have been gradually applied in the fields of standard source, local oscillation source, rapid detection, wireless signal transmission, and imaging.[3–8] Starting from the working principle of the two devices, the research progress of terahertz QCLs and QWPs is presented in this paper. The working performance of terahertz QCL based on the main material system has been improved with the development of active region structures and waveguide structures. Then, the research progress of devices based on other material systems is introduced. About the terahertz QWPs, the research progress of active regions is mainly introduced, followed by a summary of the improvement of coupling waveguide structure on device performance. The applications of the two devices in terahertz photoelectric characterization and imaging are also introduced. Finally, the improvements of the QCL-based sources and the QWP-based detectors in practical application are discussed.

2. Research status

When the working principle has been selected, the performance of the semiconductor devices mainly depends on the materials, device structure, and the level of device fabrication process. In the following, the research statuses of terahertz QCLs and terahertz QWPs are introduced respectively in details in terms of device principle, structure, and performance.

2.1. Terahertz QCLs

Terahertz QCL is a very important compact laser source in the 1–5 THz region. It has the advantages of large tunability and high energy conversion efficiency. Since its first demonstration in 2002,[1] the terahertz QCL has developed rapidly in lasing frequency, operating temperature, output power, laser beam improvement, and device stability.[7] For example, the maximum operating temperature of the device has increased from the initial 40 K to 210.5 K,[9] and the maximum pulse output power reaches watt level.[10,11] In the continuous wave (CW) mode, the highest operating temperature is 129 K,[12] and the maximum output power is 230 mW.[13] For the purpose of beam improvement, a super hemispherical lens is used to reduce the beam divergence angle to less than 3°,[10] and a small built-in reflected mirror is used to realize a terahertz beam with divergence less than 2°.[8] Figure 1 shows the progress of the maximum pulse mode and CW mode operation temperature in recent years.

In practical modules, the maximum effective output power of terahertz laser source is greater than 4 mW with the Stirling cooler and greater than 1 mW with the liquid nitrogen dewar, which fully meets the system application requirement within a certain distance.[7] In addition, the terahertz QCL has been proved to have a sub kHz quantum noise line

*Project supported by the National Key R&D Program of China (Grant No. 2017YFA0701005), the National Natural Science Foundation of China (Grant Nos. 61927813, 61775229, 61704181, and 61991432), and the Shanghai International Cooperation Project, China (Grant No. 18590780100).

†Corresponding author. E-mail: jccao@mail.sim.ac.cn

width limit,[14] and has been applied in terahertz optical comb, fine spectroscopy, and multicolor imaging.[15–17] The best performance without magnetic field of GaAs/AlGaAs-based terahertz QCLs by now is shown in Table 1. In general, the radiation power of terahertz QCLs far exceeds that of optical pumped terahertz sources and thermal radiation sources in device performance (see Table 2), and it has more advantages in building compact terahertz photoelectric test system and application system compared with huge and expensive ultrafast laser source or gas laser.[8,18]

Table 1. The progress of GaAs/AlGaAs-based terahertz QCLs.

Year	Progress	Values	Ref.
2002	the first terahertz QCL with chirped superlattice active region	4.4 THz	[1]
2003	the first bound-to-continuum structure	3.4 THz	[4]
2003	the first resonant-phonon-assisted structure	3.4 THz	[4]
2004	the first hybrid 'interlaced' design	3.75 THz	[4]
2006	minimum operating frequency	1.2 THz	[4]
2012	maximum operating frequency	5.2 THz	[4]
2014	maximum CW operating temperature	129 K/−144 °C	[12]
2016	maximum CW power	230 mW	[13]
2017	maximum pulse power	2.4 W	[11]
2019	maximum pulse operating temperature	210.5 K/−62.5 °C	[9]
2019	minimum divergence angle	1.86°	[8]

Table 2. Comparison of radiation power of terahertz sources.

Radiation type	Output power level	Ref.
terahertz QCL	> 2 W in pulse mode	[11]
	> 200 mW in CW mode	[13]
CO_2 laser pumped terahertz gas laser	> 100 mW in CW mode	[3]
free electron laser	10 W (average power)	[3]
Gobar (thermal source)	μW in terahertz range	[3]
black body (thermal source)	μW in terahertz range	[3]
photoconductive antenna	100 μW (average power)	[3]
optical difference frequency	100 μW (average power)	[3]

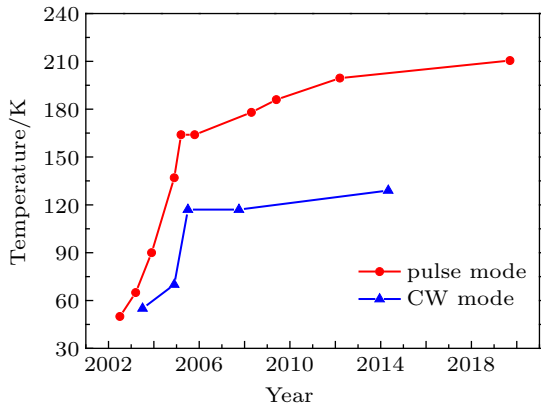

Fig. 1. Progress of the maximum operation temperature in pulse mode (red) and CW mode (blue).

2.1.1. Working principle of terahertz QCL

The working principle of terahertz QCL is shown in Fig. 2. The gain medium in the device is composed of about 200 layers of alternating semiconductor thin layer materials.

Taking the GaAs/AlGaAs material system as an example, the quantum well region in these thin layer structures is GaAs material, and the barrier region is AlGaAs material, which is grown by molecular beam epitaxy (MBE) system. In this gain medium, which we also call 'active region', the electrons are confined to separate sub energy levels. These thin layers form periodic modules. When an external electric field is applied, electrons move from one cycle to another in a cascade manner, and each step radiates a low-energy photon (see Fig. 2), where N represents the number of periods. Photons radiated from multiple cycles are gathered together in a cascade manner, and gain continuously in the cavity formed by the device ridge, and then form radiation output. The photon energy emitted is not determined by the band gap of the material, but by controlling the thickness of the semiconductor thin layer in a wide range of numerical values.[4] According to the principle of terahertz QCL, the device structure can be designed on demand. According to the designed electron transition energy difference, the frequency or wavelength of photons radiated by the device can be obtained.

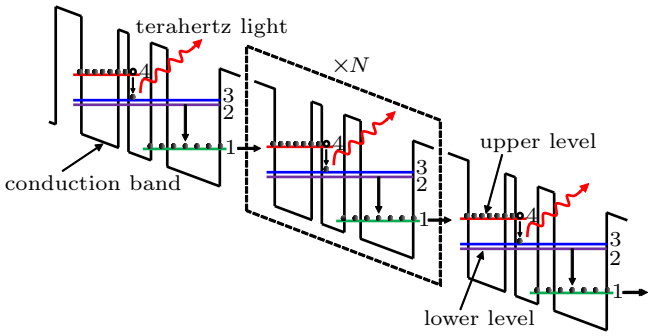

Fig. 2. Schematic diagram of working principle of terahertz QCL.

2.1.2. Active region and theoretical design

According to the different electronic transition modes, the active region of the laser can be divided into chirped superlattice, bound-to-continuum, resonant phonon, and hybrid structure.[19,20] In the first two designs, the inversion of particle number is established by the fast transmission of electrons in the miniband of superlattice. In these designs, the electrons in the device structure are well controlled, which can produce high injection efficiency, high internal quantum efficiency, and low threshold current density. However, with the increase of temperature, the miniband becomes the main channel without radiation combination, which limits the thermal performance of the two designs. In resonant phonon design, population inversion is realized by phonon assisted scattering and resonant tunneling. The removal of particles in the lower laser energy level is not sensitive to temperature, so these devices can work at a higher temperature. However, the carrier transport in this design is not well controlled, and the parasitic current is very large, so the threshold is usually very high. Because of the use of diagonal transition in the case of resonant phonon structure,[21] the threshold value is reduced by half, which is

the active region with the highest operating temperature without the help of a magnetic field.

The active region of the first terahertz QCL is a chirped superlattice structure. The device works in a pulsed mode with a lasing frequency of 4.4 THz, a pulse output power greater than 2 mW, a threshold current density of 300 A/cm^2, and a maximum operating temperature of 50 K.[1] Subsequently, there has been great progress with this device in the active regions. In 2003, Williams *et al.*[22] showed a terahertz QCL based on resonant-phonon structure, in which the inversion of particle number is realized by longitudinal optical (LO) phonon scattering. This structure is not sensitive to the temperature and distribution of electrons, and also suppresses the influence of background radiation, which is very beneficial to long wavelength and high temperature operation. The lasing frequency of the device is 3.4 THz. The working threshold at 5 K is 840 A/cm^2. In 2005, Faist's group[23] proved an improved bound-to-continuum terahertz QCL. The highest operating temperature of the device is 53 K (CW) or 116 K (pulse), and the lasing frequency of the device is 3.66 THz (82 μm). This structure has the characteristics of bound-to-continuum and phonon-assisted structure. In 2005, Liu and Cao[20,24] also showed the resonant-phonon terahertz QCL, and studied the influence of doping on the active region. The lasing frequency of the device is 2.9 THz, and the maximum operating temperature is 125 K. The results show that the operating threshold of the device rises with the increase of the doping density and decreases with the shortening of the device length. In 2006, Kumar *et al.*[25] designed a single well injected terahertz QCL. The free carrier absorption of the device is greatly reduced. The maximum operating temperature of the device is 95 K (CW) or 110 K (pulse), and the lasing frequency is 1.86 THz (161 μm). In the one-well structure, there is no extra subband, so the reabsorption between subbands is reduced. In 2006, Worral *et al.* demonstrated a bound-to-continuum terahertz QCL working at 2.0 THz. The material used is GaAs/$Al_{0.1}Ga_{0.9}$As, the threshold value is 115 A/cm^2 at 4 K, and the maximum working temperature is 47 K (CW) or 77 K (pulse).[26] With regards to theoretical design, Lü and Cao used Monte Carlo (MC) method to simulate the influence of non-equilibrium LO phonon on the electron transport in terahertz QCL,[27] and the non-equilibrium LO phonon affects the interaction between electrons and phonons in terahertz QCLs, which can change the distribution of current carriers in each subband. In 2007, Faist's group[19] demonstrated a terahertz QCL working at 1.2–1.3 THz (167–188 μm), the lowest laser frequency ever achieved without the help of a magnetic field. In 2008, Li and Cao *et al.*[28] used MC method to simulate the carrier transport and output characteristics of terahertz QCL with resonant-phonon structure.

Tunable terahertz QCL is particularly important for the development of terahertz applications. In 2008, Freeman *et al.* proposed a kind of non-uniform cascade active region to realize the electric switch emission of terahertz QCL[29] with a bound-to-continuum structure. The laser frequency is 2.6 THz and 3.0 THz, and the operating temperature is 60 K and 91 K, respectively. In the former mode, the device threshold is 79 A/cm^2. Compared with selective injection,[30] the above two modes can be switched without magnetic field. In 2009, Kumar *et al.*[31] developed a double-well terahertz QCL. Only three subbands participate in electron transport. The laser frequency is 4.6 THz, and the threshold value is 350 A/cm^2. In the same year, Wade *et al.* realized the laser emission of a single device in a wide frequency range (0.68–3.33 THz) by applying an appropriate bias voltage and a strong magnetic field of more than 16 T.[32] Due to the suppression of non-radiation scattering between Landau energy levels, the device showed the magnetic field assisted laser effect when it was working. The maximum operating temperatures of the device at 1 THz and 3 THz were 215 K and 225 K, respectively. In 2009, the same research group adopted the improved resonant-phonon structure. The diagonal transition was used to extend the lifetime of the upper lasing level, so that the working temperature of the device is increased to 186 K, the laser frequency is 3.9 THz, and the output power is 63 mW at 5 K and 5 mW at 180 K.[21] In 2009, Kumar *et al.* used the density matrix method to study the resonant tunneling mechanism.[33] Based on the previous work, Freeman *et al.*[34] developed a dual wavelength terahertz QCL in 2010, which emits at 2.5 THz and 2.9 THz using non-uniform active region. In the same year, Kumar *et al.* designed a four-well scattering assisted terahertz QCL, providing a breakthrough in terahertz QCL's operating temperature. This 1.8-THz laser can work up to 163 K, corresponding to 1.9 times of $\hbar\omega/k_B$.[35] This development is attractive for QCL applications below 2 THz, and brings forward a new design idea for realizing the room temperature terahertz semiconductor laser.

In practical application, due to the severe absorption by water, the water vapor in both the optical system and the sample will attenuate the energy of terahertz radiation. Therefore, the development of high-power terahertz QCL technology has become a research hotspot in this field. The following is a detailed introduction from the perspective of active regions. In 2006, Williams *et al.* used a four-well resonant-phonon structure with resonant tunneling and phonon scattering mechanism to realize a terahertz QCL with a lasing frequency of 4.4 THz, a maximum pulse power of 248 mW, and a maximum continuous wave power of 138 mW.[36] In addition to optimizing the active region to improve the device gain, the output power of the device can be further improved by increasing the thickness of the active region or increasing the size of the cav-

ity. In 2013, Brandstetter *et al.* used a symmetrical active region to increase the thickness of the active region to 20 μm by directly bonding two pieces of device materials, and made a semi insulating surface plasmon (SI-SP) waveguide QCL device emitting at 3.9 THz, achieving a peak power of 470 mW at one facet.[37] However, the realization of this bonding technique requires the precondition that the active region must be symmetrical and the quality of wafer bonding is very high. In 2014, Li *et al.* hybridized the bound-to-continuum structure and the resonant-phonon structure, resulting in a new type of active region, i.e., the hybrid structure. At the same time, they used a larger size of the resonator and the rear face coating technique to improve the output power of terahertz QCL. The maximum pulse peak power of 1.01 W is achieved with the device size of 4.2 mm × 425 μm,[20] and the device lasing frequency is 3.4 THz. In 2015, by precisely controlling the growth rate and doping level of the material, Li *et al.* realized the layer by layer growth reproduction of the laser material. Using the optimized structure and doping concentration, the high-power ridge device was prepared, and the terahertz QCL with the maximum pulse output power of 1.56 W (two-facet) was realized.[38] In 2017, Li *et al.* borrowed the previous bonding technique to increase the thickness of the active region. Through exquisite material growth technique, the thickness of the active region was directly grown to twice of the conventional thickness, i.e., 24 μm. The rear face coating and large-size ridge device were also used to obtain the maximum 2.4 W pulse peak power,[11] and the device lasing frequency was 4.4 THz. In 2018, Wan *et al.* realized a terahertz QCL with peak pulse power of 1.2 W and lasing frequency of 4.3 THz[10] by using a single resonant-phonon structure. With regards to continuous wave output power improvement, in 2016, Wang *et al.* developed a CW high power terahertz QCL on the basis of hybrid structure. The maximum output power is 0.23 W, and the lasing frequency is 3.11 THz.[13]

2.1.3. Device materials

In addition to the above terahertz QCLs based on GaAs/AlGaAs material system, scientists have also studied the method and feasibility of realizing terahertz QCLs on several other material systems.

In the InGaAs/AlInAs/InP material system, the effective mass of electron is small, which can greatly improve the oscillation intensity, reduce the influence of surface roughness, weaken the interaction between electron and phonon, and thus reduce the threshold current density. However, InP-based materials are not developed as mature as GaAs-based materials in terms of device performance and epitaxial growth. Therefore, compared with GaAs-based terahertz QCLs, InP-based terahertz QCLs still need to be further improved in output power, operating temperature, etc. In 2005, the Faist group carried out the terahertz QCL research based on InGaAs/AlInAs/InP, and obtained the emission frequency of 3.6 THz and the highest working temperature of 45 K. The device threshold current density was 460 A/cm^2 at 10 K.[39] In 2009, the team also developed a terahertz QCL of $In_{0.53}Ga_{0.47}As/In_{0.52}Al_{0.48}As/InP$, with lasing frequency of 3.75 THz (80 μm), maximum operating temperature of 63 K and 87 K in continuous mode and pulse mode, respectively, and maximum output power of 4 mW@10 K.[40] In 2012, based on the three-well phonon depletion scheme, Deutsch *et al.* successfully developed the terahertz QCL with a maximum operating temperature of 142 K by using the $In_{0.53}Ga_{0.47}As/GaAs_{0.51}Sb_{0.49}$ material matched with InP substrate. The advantage of this device is that it improves the injection and extraction tunneling coupling in the device. The threshold current density of the device is 0.75 kA/cm^2, and the peak pulse power can reach 9 mW. The wide spectral emission range between 3.3 THz and 4 THz was also measured.[41] In 2017, the group also used InGaAs/InAIAs materials with low effective electron mass to develop the high-power terahertz QCLs. The research shows that the interface roughness, the doping migration, and the growth-related asymmetries of the device materials play important roles in the material system. The analysis shows that the doping densities are 2×10^{10} cm^{-2} and 7.3×10^{10} cm^{-2} respectively corresponding to the conditions that the device working at the highest temperature (155 K) and at the highest pulse power (151 mW). In addition, by connecting the super hemispherical GaAs lens to the device with the highest doping level, the output power of the device is 587 mW.[42]

In the GaN/AlGaN material system, it is expected to further improve the operating temperature of terahertz QCL, and even achieve room temperature operation, thanks to its higher longitudinal optical phonon energy than GaAs/AlGaAs material. In 2005, Vukmirović *et al.* studied the terahertz quantum-well structure of GaN/AlGaN theoretically. The simulation results show that the above structure can be excited at 8.33 THz (36 μm).[43] In 2008, Bellotti *et al.* simulated the terahertz QCLs based on GaN using MC method, and its lasering frequency was 2.0 THz.[44] Compared with the GaAs-based terahertz QCLs, the GaN-based devices have excellent thermal performance, and the maximum operating temperature can reach to 400 K. However, due to the lack of high quality GaN substrate and epitaxial materials, it is still very difficult to grow such materials by MBE system. In 2015, Terashima *et al.* announced that they had successfully developed the GaN-based terahertz QCL[45] at a SPIE conference, with lasing frequencies of 5.5 THz and 7.0 THz, which, however, has not been repeated by other research groups in the world to date. Scientists with different opinions argued that the laser developed by that group is not the QCL in real sense,

but may be the radiation generated by the electronic transition of impurity level in GaN material.

In other wide band gap semiconductor materials, in 2006, Popadic *et al.* proposed an optical pumped laser based on ZnSe/$Zn_{1-y}Cd_ySe$ double quantum-well structure and $Zn_{1-x}Mn_xSe$ diluted magnetic semiconductor barrier,[46] with a tunable frequency of 4.17 THz–5.0 THz (corresponding wavelength of 60–72 μm). In this design, the diluted magnetic parts of different subbands and structures overlap with each other. The giant Zeeman splitting in the diluted magnetic semiconductor results in the splitting of the electronic state, which leads to the tuning of the external magnetic field to the laser wavelength. In 2009, Bellotti *et al.* simulated the terahertz QCL based on ZnO/MgZnO material system, and found that this device may work at high temperature.[47] However, these two kinds of terahertz QCLs need magnetic field in operation, which greatly limits the application of this device.

With regards to Si-based materials, in 2002, Lynch *et al.*[48] carried out the optimization design of terahertz QCLs based on Si/SiGe and Ge/SiGe materials, using the transitions from heavy-hole to heavy-hole and from light-hole to heavy-hole to emit terahertz light. In 2008, Lever *et al.*[49] studied n-type doped Si–SiGe terahertz QCLs by employing the rate equation considering the surface roughness, carrier-phonon scattering, and Coulomb interaction. The simulation results show that the lasing frequency of the device is 3.6 THz, and the threshold current density is about 70 A/cm^2. For the above-mentioned Si-based terahertz QCLs, the polarized optical phonon scattering could be omitted, and good thermal performance has been observed, which is expected to work at room temperature. Mature and cheap silicon preparation technology also makes the above-mentioned devices be easily used in the integration of other microelectronic devices. However, Si-based terahertz QCLs also have their own problems, such as the serious interaction between the hole subbands and the relative effective mass of the hole being much larger than that of the electron,[50] thus affecting the actual performance of the device.

2.1.4. Waveguide structures

According to the different types of waveguide structures, the terahertz QCLs can be divided into two types: semi-insulating (SI) surface plasmon (SP) waveguide and metal–metal (MM) waveguide,[19,51] as shown in Fig. 3. The lasing wavelength of the device is typically 100 μm (3 THz), and the thickness of the active region of the device is usually only 10–15 μm. As a consequence, there is diffraction effect when the light emitting from the ridge facet of the device, and the light beam is relatively divergent.

In SI-SP waveguide, n-type doped GaAs substrate is replaced by SI-GaAs substrate to reduce free carrier absorption. A thin heavily doped layer (200–800 nm in width) is grown on SI-GaAs substrate to form the plasma layer. Terahertz light is confined between the top metal contact layer and the bottom plasma layer, reducing the overlap between the mode and heavily doped semiconductor, thus reducing the free carrier absorption and waveguide loss. The MM waveguide eliminates the limit and reduces the threshold greatly. The fabrication of this waveguide is more complicated resulting from the needs of metal–metal or metal–semiconductor bonding. At present, the MM-waveguide based terahertz QCLs have the best performance owing to the small skin depth in metal and the confinement factor is almost uniform. In recent years, the studies of terahertz QCL have made rapid progress in the new type waveguide structure, such as grating, photonic crystal, and metasurface, which makes the divergence and inhomogeneous distribution of the light beam greatly improved.

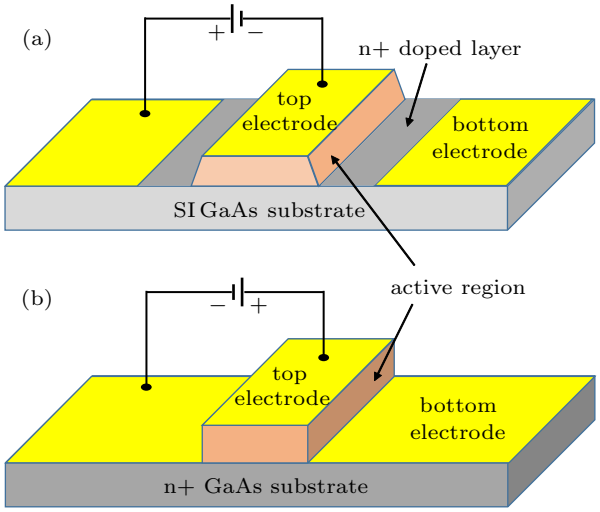

Fig. 3. Schematic diagram for (a) SI-SP and (b) MM waveguides.

For the terahertz QCLs with grating structure, the Bragg grating with periodic structure is usually used. The main function of grating is to realize the feedback of light. Only the light fulfilling the Bragg condition can be reflected and strengthened, and the coupling between forward and backward waves can be obtained to realize the longitudinal mode selection. Therefore, we call it the distributed feedback (DFB) structure. The DFB lasers with the Bragg grating are superior to the traditional Fabri–Pérot (F–P) cavity laser in monochromaticity and stability, and the order of the grating determines the direction of the output light. The second-order grating is introduced into the terahertz QCL, and the laser oscillates along the length of the cavity and emits along the vertical direction of the device surface. For example, the advantage of the second-order grating surface emitting DFB terahertz QCL is that the output area increases and the far-field divergence performance of the laser is improved. There are symmetric modes corresponding to the bottom of conduction band and antisymmetric modes

corresponding to the top of valence band in the second-order DFB laser. The symmetrical mode can radiate electromagnetic wave from grating slot, but the antisymmetric mode radiation is very weak. Due to the small radiation loss of antisymmetric mode, the laser is easier to excite when it is working, which also leads to the low output power of the laser and the shortage of two spots in the far field. It is necessary to introduce π-phase shift to obtain a single far field spot.[52] The introduction of third-order grating, antenna feedback plasma grating, and line DFB grating has the similar effect with the phased array in millimeter wave devices, which can realize the phase-locked effect and form a narrow beam with low divergence. The introduction of two-dimensional (2D) photons into the terahertz QCLs waveguide is mainly for the purpose of better controlling the divergence of the laser beam from two dimensions and obtaining an ideal Gaussian beam. Therefore, some 2D photonic structures such as concentric-circle grating, annular grating, (quasi) photonic crystal, and random structure are used in the waveguides of terahertz QCLs. In addition, the fabrication of two-dimensional photonic crystal structure on the surface of metal waveguide can also improve the far-field performance of the laser. Furthermore, in order to achieve single-mode, narrow collimated beam, high output power, polarization controllability, and tunability on terahertz QCLs, the structure of vertical external cavity surface emitting laser (VECSEL) together with the metasurface structure is employed. The research progress of terahertz QCLs in waveguide structures is as follows.

In 2005, Hu's group significantly improved the confinement factor by employing the millimeter size waveguide to confine the optical mode. At the same time, Cu–Cu bonding was used instead of In–Au bonding to improve the temperature performance of the device. The maximum temperature of the device was 164 K (pulse) or 117 K (CW),[53] the laser frequency was 3.0 THz, the calculated confinement factor was 0.93, and the loss was about 18.7 cm^{-1}. In the same year, using microcavity terahertz QCL at 3.0 THz–3.8 THz, Fasching *et al.* demonstrated a kind of low divergence beam laser,[54] with a maximum operating temperature of 140 K and a minimum threshold of 0.9 kA/cm^2. In 2006, Cao's group optimized the resonant-phonon structure at 3.1 THz and 3.4 THz by MC method, and realized the high-quality growth of device materials. The devices with SI-SP waveguide and MM waveguide were prepared. The successively measured results showed that the lasing frequency of SI-SP waveguide device was 3.2 THz,[55] and that of MM waveguide device was 3.39 THz, operating at temperature up to 100 K.[56] In 2007, Faist's group proposed to combine photonic crystal and MM waveguide to improve the performance of terahertz QCLs. The research results show that under the condition of strong magnetic field and low temperature, the device threshold can be reduced to 0.65 A/cm^2.[57] Subsequently, the studies of Benz *et al.*[58] also show that for terahertz QCL with photonic crystal structure, the reflectivity is improved owing to the lasing frequency in the photonic band gap, which helps to reduce the loss. In 2010, Fast's group also demonstrated a low divergence terahertz photonic-wire laser with a very small structure. The emission is concentrated in a narrow beam. The maximum operating temperature is 110 K in CW mode, the output power is greater than 10 mW, and the slope efficiency of the laser at 10 K is 200 mW/A.[59] Meanwhile, they also proposed a surface emission distribution feedback terahertz laser resonator based on a dual-slit configuration.[60] The first-order and second-order diffractions can be well controlled by the gap spacing, so the surface loss can be selected in a large range. In 2010, Yu *et al.* designed a sub wavelength periodic structure at the facet of the laser, which significantly reduced the asymptotic surface plasmon frequency, leading to 'spoof' surface plasmons. Using a simple one-dimensional grating design, the divergence angle of the laser beam was reduced from about 180° to about 10°, the directivity was improved by more than 10 dB, and the power collection efficiency was about 6 times higher than that without optimization.[61] Subsequently, Xu *et al.* proposed a graded photon heterojunction grating structure, which has a decreasing metal filling ratio from the center to both sides.[62,63] This grating can limit the symmetric mode to the middle of the waveguide and the antisymmetric mode to both ends of the waveguide. Through the above structure, the device is forced to work in the symmetrical mode to improve the optical efficiency. Compared with DFB laser, the slope efficiency of the laser is increased by an order of magnitude, and the far field presents a single elliptical Gaussian spot with low scattering.[62] In 2018, Jin *et al.* adopted the asymmetric second-order and fourth-order hybrid grating DFB structure, which greatly increased the output power of the laser.[64] This hybrid structure is based on the second-order grating, adding the asymmetric fourth-order grating, so as to reduce the loss of the symmetrical mode (corresponding to the excited state of the laser) and greatly increase the radiation efficiency of the laser. At 62 K, the maximum output power of the device is 170 mW, and the far field is a single elliptical spot. Different from the surface emitting mechanism of the second-order grating, Amanti *et al.*[65] proposed a kind of terahertz QCL based on the third-order grating, which is similar to the linear phase controlled source array, and can shape the far-field of the double-sided metal waveguide divergence into a single beam with only 10°. The output power is 7 times of that of the double-sided metal waveguide device with the same area. In 2016, Wu *et al.* demonstrated an antenna feedback plasmon terahertz QCL.[66] The grating period is no longer a multiple of the half wavelength of the laser in the active region, but between the first-order and second-order

grating periods. Through the selection of a specific grating period, the electromagnetic field in the resonant cavity strongly couples with the surface plasmon field in the air outside the cavity. The gratings are similar to the antenna array to form a phase-locked terahertz field distribution, thus generating narrow beams along the waveguide in both directions. This antenna feedback mechanism can effectively control the divergence of the light, and realize a very narrow light beam with divergence of only $4^\circ \times 4^\circ$. In 2018, Biasco *et al.* proposed a line DFB terahertz QCL,[67] in which the optical feedback is provided by sinusoidal corrugated gratings on both sides of the resonator. A low scattering single-mode light beam with a peak power of about 42 mW and a slope efficiency of about 250 mW/A is obtained.

With regards to 2D photonic crystal structure, in 2009, Mujagić *et al.* proposed a surface emitting annular grating structure.[68] This grating is equivalent to the bending end-to-end connection of 1D linear grating, and the laser works in a whispering-gallery mode, which has strong beam collimation effect, and the far-field spot is symmetrical and approximately circular. The radiation efficiency is twice of that for F–P laser with the same area. In addition, the laser always operates in single-mode, and the edge mode rejection ratio is higher than 30 dB. In the same year, Chassagneux *et al.* developed the photonic crystal surface emitting terahertz QCL, and studied the influence of boundary conditions on the photonic crystal.[69] In 2010, Sevin *et al.* improved the above terahertz QCLs. The quality factor of the resonator is improved by employing the gradual photonic crystal structure, which can greatly reduce the device area[70] without affecting the divergence of the beam, and then the π phase shift was introduced to obtain a single narrow beam. The divergence angles of both dimensions are about 10°. In 2013, Liang *et al.* realized the surface emitting in single-mode[71] by employing the distributed feedback concentric circular gratings. The edge mode rejection ratio of the laser is as high as 30 dB, and the output power is 5 times that of the edge emitting laser with the same size. In 2014, Vitiello *et al.* developed the photonic quasicrystal terahertz QCL[72] by using the pentagonal rotationally symmetric quasicrystal structure. The laser works in the mode corresponding to the quasicrystal structure. Compared with the photonic crystal devices, the photonic quasicrystal terahertz QCLs have higher output power and optical efficiency. Random laser is a fed back laser by multiple elastic scattering in a highly disordered environment. Because of its low spatial coherence, it can provide an ideal light source for non-artifact imaging. In 2019, Biasco *et al.* realized the terahertz QCL[73] with random structure, in which air holes are randomly distributed on the upper surface of the waveguide, resulting in a highly collimated vertical surface emitting terahertz laser. In addition, the external cavity composed of a movable mirror is used to adjust the laser frequency, and a continuous frequency tuning of more than 11 GHz is acquired.

About metasurface structures, in 2015, Xu *et al.* realized the terahertz VECSEL[74] by employing an amplified subsurface reflector composed of antenna coupled quantum-cascade subcavity arrays. The laser consists of metasurface reflector and output coupler. The period interval of the double-sided ridge waveguide array is less than the wavelength in free space, and the width of the ridge waveguide is about half wavelength in the active region. The lasing mode is a high-order transverse mode TM_{01}. Using this structure, a collimated beam with a quality close to Gaussian is obtained. The full width of the half peak is $4.3^\circ \times 5.1^\circ$, and the output power of the laser is greater than 5 mW. In 2018, Curwen *et al.* developed a high-power terahertz VECSEL[75] by employing the optimized terahertz quantum-cascade metasurface, which is composed of double-sided metal ridge waveguide array, including terahertz quantum-cascade material and metal-grid-based output coupler. The output power per unit area increases with the rising spatial density of metasurface structure. In order to obtain an ideal Gaussian beam, a circular bias region is confined for the ridged waveguide array by using the dielectric layer. The output power of the device can reach to 1.35 W at 6 K, and it has the characteristics of single-mode and perfect circular spot with low divergence. In addition, the single-mode terahertz laser can be continuously tuned with a frequency width of 50 GHz by controlling the length of the cavity, and the single-mode tuning does not significantly affect the output power or beam quality.

The dynamic control of polarization state in the laser is very important for polarization imaging, polarization spectroscopy, ellipsometry, etc. In 2017, Xu *et al.* realized the direct electric control of the polarization state of the light in terahertz laser by employing a metasurface structure.[76] The polarization-sensitive metasurface is composed of two different surface emitting antenna arrays with Z-shaped ridge waveguide. When a bias is applied to the array, a certain polarization state will be selected. The above structure realizes the electric switch between 80° linear polarization state, and also a very narrow beam is kept. The divergence angle is about $3^\circ \times 3^\circ$. The metasurface structure also plays an important role in the tunability of terahertz QCLs. Because of the gain of VECSEL device comes from the metasurface reflector, which does not involve the middle of the cavity, the short cavity structure is beneficial to the realization of wide-spectrum tunability of the laser. In 2018, Curwen *et al.* employed the short cavity structure to make the laser oscillate in the low-order F–P cavity mode. By mechanically controlling the coupler to change the cavity length, a single-mode terahertz VECSEL with continuous tunaility in a wide spectral range[77] was realized. The lasing frequency is 3.5 THz. When the order of the longitu-

dinal mode of the external cavity is 4, the continuous tunable bandwidth reaches to 650 GHz, and the tuning range is about 19% of the center frequency. When the order of the longitudinal mode of the external cavity is 2, the tunable bandwidth reaches to 880 GHz, and the tuning range is about 25% of the center frequency. If one can control the phase of the metasurface and the output coupler, and develop a thinner metasurface structure at the same time, it is expected to achieve the first-order external cavity longitudinal mode tunability, and further improve the operation bandwidth of the device.

2.2. Terahertz QWPs

Terahertz QWP[2] is a kind of low dimensional semiconductor quantum device working in terahertz region. Its effective detection frequency range can cover 1.5 THz–7.5 THz and 8.8 THz–15 THz. This kind of detector has the advantages of simple structure, fast response, stable performance, easy integration, and high damage threshold, making it especially suitable for high-speed detection and high-speed imaging applications.[8] As with terahertz QCL, the material system used in terahertz QWP is GaAs/AlGaAs. However, due to the low energy of the terahertz photon, which corresponds to the low Al concentration in the material, the growth of high-quality GaAs/AlGaAs material is extremely difficult. Starting from the principle, the research progress in theoretical design, structural optimization, and performance improvement of the device is presented.

2.2.1. Working principle

Terahertz QWP is the extension of quantum-well infrared photodetector (QWIP) to terahertz frequencies, and they are similar in both working principle and device characteristics. The conduction band structure and working principle diagram of the device are shown in Fig. 4.

The periodic structure composed of multiple quantum wells and barriers as well as the upper and lower contact layers constitute the active region of the device. Each period contains a layer of doped quantum-well layer (GaAs) and a layer of barrier layer (AlGaAs). When the terahertz radiation incidents on the sensitive facet of the device, the electrons located in the bound state of the quantum well will absorb the photon energy and then transit to the quasi-continuous state near the barrier edge. Under the external bias, the photo-carriers (electrons) form a photocurrent in a specific direction. The intensity of the incident light radiation can be obtained by measuring and analyzing the magnitude of the photocurrent. Then the terahertz light is detected. The peak response frequency of the device is determined by the energy interval from the bound state to the quasi-continuous state in the structure. The energy interval can be changed by adjusting the height of the barrier, the quantum-well width, and the doping concentration in the active region, so as to realize the on-demand design. In order to ensure the full absorption of the incident light, the number of periods in the active region is usually 10–100.[78]

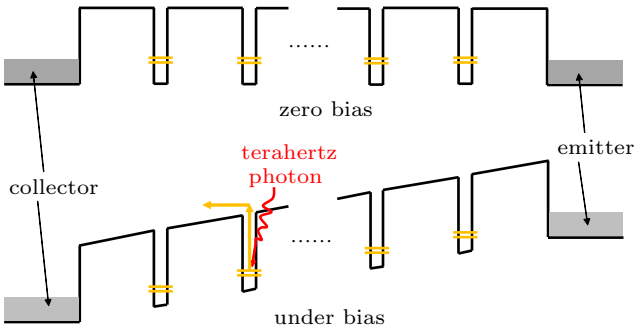

Fig. 4. Schematic conduction band edge profile of a GaAs/AlGaAs terahertz QWP under zero (above) and finite (below) bias.

2.2.2. Research progress

The terahertz QWP was first developed by Liu *et al.* in 2004.[1] Most important progresses have been made in theoretical design,[79–82] coupling waveguide,[83–85] and system applications[86–89] in recent years.

In theoretical design, in 2009, by considering the influence of many-body effect in the device, three different peak detection frequencies were calculated and fitted by Guo *et al.* The results show that the influence of the peak detection frequency in terahertz detectors with many-body effect is far greater than that in infrared devices, which reduces the design error of the peak detection frequency from 30% to 5%, greatly improving the theoretical design accuracy of terahertz QWP.[79] In 2015, Gu *et al.*[90] found a strong and sharp photocurrent peak at the longitudinal optical (LO) phonon frequency (8.87 THz). The results show that the peak value of photocurrent comes from a two-step process. Firstly, at the LO phonon frequency, a large number of unbalanced LO phonons are excited by the incident electromagnetic field, which makes the electromagnetic energy localized and enhanced in the thin multi-quantum-well (MQW) layer. Secondly, through the Frohlich interaction, the local electrons are excited to a continuous state by absorbing the non-equilibrium LO phonon, thus producing a strong light response peak. This discovery is of great significance for the exploration of strong light–matter interaction and the realization of high sensitivity terahertz photodetectors. About improving the coupling efficiency and responsivity of the detectors, in 2013, Guo *et al.* studied the effect of the surface-plasmon enhanced grating structure and the metal microcavity structure in improving the coupling efficiency of detectors. The theoretical results show that the surface plasmon enhanced grating structure can increase the coupling efficiency by 30 times, and the metal microcavity structure can reach to 100 times.[81] In 2014, Zhang *et al.* developed a terahertz QWP based on the coupling of 1D metal grating. The results show that the peak responsivity of the device

can be effectively increased by 20%.[91] In 2015, a 5.0 THz patch antenna terahertz QWP was demonstrated by Palaferri *et al.*[92] A peak detectivity of 5×10^{12} cm·Hz$^{1/2}$/W was realized. In 2017, Zhang *et al.* designed a device based on 2D metal grating structure, and developed a terahertz QWP device with a responsivity of 146% higher than the traditional 45° facet incident structure.[85] In 2017, Wang *et al.*[93] designed and developed a two-color terahertz QWP with peak detection frequencies of 3.75 THz and 5.55 THz, respectively. The response width of the photocurrent spectrum is about 1.5 THz at half maximum intensity. In 2018, Wang *et al.*[94] demonstrated a broadband voltage-regulated terahertz QWP. The peak detection frequency can be regulated from 4.5 THz to 6.5 THz. In addition, in 2015, Schneider's group demonstrated a two-photon terahertz QWP below 6 THz, and used the terahertz gas laser to study the nonlinear performance of the detector.[84] In operation temperature, in 2015, Jia *et al.* found that when a terahertz light beam with a power density of 819 W/cm^2 is introduced, the optical-noise-limit performance temperature of the terahertz QWP with a peak detection frequency of 5.5 THz can be increased to over 77 K,[82] which provides guidance and help for improving the operating temperature of terahertz QWP. The plasmon resonant[95] and the mico-cavity coupled[96] terahertz QWPs were realized by Zheng *et al.* and designed by Yang *et al.*, respectively. Finally, the progress of the performance of terahertz QWPs is shown in Table 3.

Table 3. The progress of GaAs/AlGaAs-based terahertz QWPs.

Year	Progress	Values	Ref.
2004	the first terahertz QWP	7.1 THz	[2]
2009	precise design of device structure	3.2 THz/5.4 THz	[79]
2013	microcavity coupled terahertz QWP	5.4 THz	[81]
2014	grating coupled terahertz QWP	5.85 THz	[91]
2015	antenna coupled terahertz QWP	5.0 THz	[92]
2015	the first two-photon terahertz QWP	6.0 THz	[84]
2017	the first two-color terahertz QWP	3.4 THz	[93]
2018	broadband bias-tunable terahertz QWP	4.5 THz–6.5 THz	[94]
2019	plasmon resonant terahertz QWP	6.5 THz	[95]

3. Applications

Terahertz QCL and QWP are spectrally matched semiconductor devices. Figure 5 shows the photocurrent spectrum of a terahertz QWP with peak detection frequency of 3.2 THz and emission spectra of five terahertz QCLs with different lasing frequencies. The spectra show that one terahertz QWP can detect radiation from almost all terahertz QCLs. With the optimization on terahertz device, the application system, employing terahertz QCL as the light source and terahertz QWP as the detector, has also been significantly developed. The research progress in terahertz photoelectric characterization and terahertz imaging employing the above two devices is mainly presented as follows.

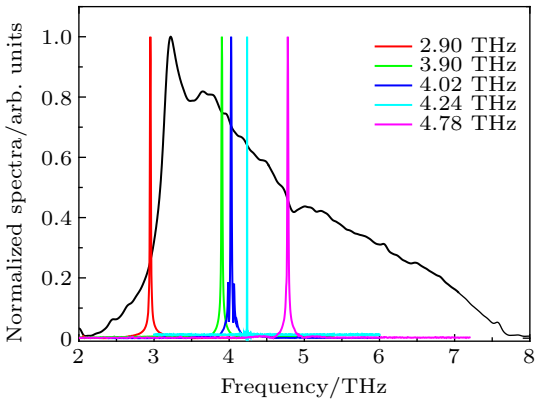

Fig. 5. The comparison of the emission spectra of five THz QCLs and the photocurrent spectrum of a THz QWP.

3.1. Terahertz photoelectric characterization

Photoelectric characterization is an important foundation in terahertz application, covering aspects such as performance characterization of terahertz photoelectric devices, optical path calibration and beam optimization, spectrum measurement, light modulation and demodulation, wireless signal transmission, etc. With the development of material science, laser technology, and energy band engineering, compact terahertz sources and detectors are gradually emerging and their performance is constantly improved. The photoelectric characterization methods in terahertz range are gradually updated, and the physical parameters that are difficult to accurately measure by traditional methods can be easily acquired. Terahertz QCL and QWP are two important devices in high frequency terahertz photoelectric characterization. They have unique characterization advantages in pulse power measurement, responsivity calibration, and fast modulation and detection.

In 2009, Grant *et al.*[86] applied terahertz QWP into a 3.8 THz wireless transmission system for the first time, demonstrated the transmission of a real-time audio signal, and realized the breakthrough of wireless signal transmission based on a radiation above 1 THz. In 2010, Tan *et al.*[97] combined the refrigerator of terahertz QWP with the spectrometer based on the Fourier transform spectrum measurement technology. A terahertz QWP device was used to detect the emission of a QCL device with lasing frequency of 4.1 THz. The results show that the emission spectrum of the laser measured by terahertz QWP is sharper than that measured by thermal detector with the same condition, which is closer to the actual emission spectrum. Then, accurate calibration of the pulse power emitting from terahertz laser was realized by Tan *et al.* by employing the fast detection performance of terahertz QWP.[98] Subsequently, the absolute responsivity of terahertz QWP was calibrated by employing a single frequency terahertz QCL, which is similar to the results in Ref. [78]. The calibration process is simple and the error is small, which ef-

fectively eliminates the calculation of complex integral difference and the influence of water vapor absorption in the atmospheric environment.[99]

In 2010, Fatholoumi *et al.*[87] used a fast terahertz QWP to study the thermal quenching process of a terahertz QCL, and the response time of the corresponding devices was in the order of microseconds. In 2011, Chen *et al.*[100] adopted a 4.1-THz CW QCL as the emitter and a spectrally matched terahertz QWP as the receiver to realize the wireless transmission of real-time audio signal. The amplitude modulation was used in the transmission process with a distance of 2 m. The modulation bandwidth limited by the device circuit is about 580 kHz. Furthermore, Chen *et al.*[101] optimized the driving circuit of terahertz QCL and the signal processing circuit of terahertz QWP.

A 3.9-THz wireless link with a distance of 2.4 m and a transmission rate of 2.5 Mbps is realized. Wireless transmission of a real-time video signal was demonstrated. The results based on the analysis of transmission of binary pseudo-random signal show that the error-free transmission rate of the link is 5 Mbps. In 2015, the wireless transmission rate had been raised to 20 Mbps by improved the digital modulation circuit and the trans-impedance amplifier. The distance of the link, with a 3.27 THz carrier frequency, is about 2.2 m. In 2017, Tan *et al.*[102] used a 4.3-THz QWP to realize the direct detection of a rapidly modulated 4.2 THz light, with the fastest response frequency of 0.5 GHz. By improving the packaging method of terahertz QWP, Li *et al.*[15] used a coaxial transmission line to extract the response signal of the detector, and finally demonstrated the direct detection of a 6.2 GHz modulated light.

In addition, the terahertz QCLs have also been applied in precision spectroscopy and optical frequency comb. In 2017, a homogeneous spectral spanning of long-cavity terahertz QCL under radio frequency modulation was demonstrated by Wan *et al.*[103] The terahertz spectrum under radio frequency modulation continuously spans 330 GHz was realized under a single drive current. In 2019, the high-power and broadband on-chip dual-comb sources based on terahertz QCLs emitting at approximately 4.2 THz were realized by Li *et al.*[104] In 2020, the practical terahertz transmission dual-comb spectroscopy with a free-running QCLs generating approximately 120 GHz wide combs centered at 4.2 THz was demonstrated by Li *et al.*[105] Spectra of moist air are shown, which allows rapid monitoring of the relative humidity. The above results show that the terahertz dual-comb technique should be readily extendable to perform imaging, microscopy, and near-field microscopy in the terahertz regime.

3.2. Terahertz imaging

With the development of terahertz source and detection technology, terahertz imaging has gone through many stages, such as the imaging based on terahertz time-domain spectroscopy (TDS) system,[106,107] fast scanning imaging based on various radiation sources,[108–111] and real-time imaging with focal plane arrays.[112,113] The performance and the application level of the imaging system have been greatly improved. It is noted that the appearance of terahertz real-time imaging system[14,115] improves the speed and accuracy of terahertz imaging to the required levels for practical applications. The terahertz imaging has important applications in material analysis, biomedical imaging, and other fields in the future. The imaging system based on terahertz QCL and QWP devices will be mainly presented as follows.

In real-time imaging based on terahertz QCL, the infrared focal plane array was employed by Lee *et al.*[113] to demonstrate the terahertz real-time imaging system in 2006, and a sub-millimeter resolution has been acquired. The light source of this imaging setup is a 4.3-THz QCL with CW mode. Then, by improving the output power and beam quality of the laser and the sensitivity of the detection array, they further realized a stand-off imaging of the pattern with the distance up to 25 m. The imaging resolution is sub-millimeter level.[116] In 2008, Oda *et al.*[114] demonstrated the real-time imaging for the first time by using an optimized terahertz imaging array. The imaging frame rate can reach to 30 Hz. The theoretical optimal imaging resolution of this system is determined by the pixel size of the terahertz array (with a value of 23.5 μm). In actual imaging systems, the resolution is determined by the wavelength of radiation, focal length of the optical lens, the material of the sample, etc. Therefore, the actual imaging resolution of the object is on the order of submillimeter. In 2012, Oda *et al.*[115] developed an optical lens suitable for terahertz array. The microscopic imaging of two hair silks, with a resolution of 70 μm, was demonstrated. It is worth noting that the imaging system uses a compact terahertz QCL device with Stirling cooler, which greatly reduces the size and weight of the system, and then improves the application scopes of the terahertz QCL. In 2014, Tan *et al.*[117] demonstrated the reflection imaging of metal patterns and concealed metal blades by employing a 3.9-THz QCL as the light source and a 320×240 terahertz camera. An imaging resolution of 0.33 mm was obtained. In 2016, Yang and Tan *et al.*[118] used a compact terahertz QCL device and a terahertz array detector to build a terahertz real-time imaging system with a light pass aperture of 50.8 mm and an imaging spot diameter of more than 40 mm. The actual imaging resolution is about millimeter level. After integration optimization, the above imaging device is applied to the imaging part of a terahertz hazardous substances analyzer. The real-time imaging and positioning of hazardous substances such as explosives have been demonstrated, which is shown in Fig. 6.

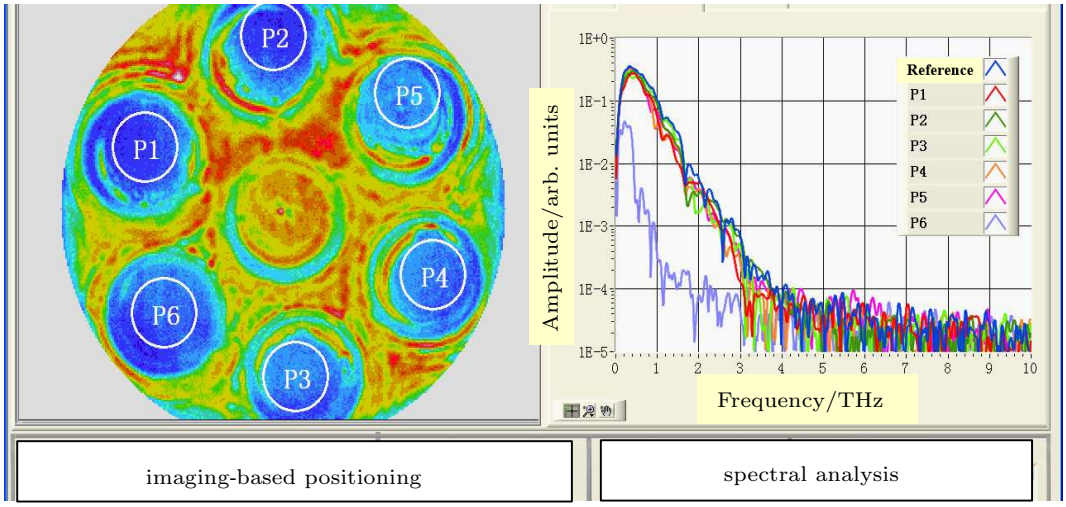

Fig. 6. The imaging, positioning, and spectral analysis process of hazardous substances.

In scanning imaging based on terahertz QCL and QWP, Zhou *et al.*[119] used a 3.2-THz QWP as the signal receiver to realize a passive terahertz scanning imaging assisted by the thermal radiation source in 2012. The imaging resolution is about 1 mm. In 2013, Tan *et al.*[88] constructed a scanning imaging system by using a 3.9-THz QCL as the light source, a spectrally-matched terahertz QWP as the signal receiver, and two ellipsoidal replica mirrors as the optics. The scanning transmission imaging of the hidden pattern in the RMB was demonstrated. The imaging resolution is 0.5 mm. In 2014, a scanning reflection imaging of the logo pattern on the U-disk surface was demonstrated by Tan *et al.*[120] employing the same light source and receiver. The imaging resolution is 0.4 mm. In order to further improve the imaging speed, in 2018, a scanning imaging system based on the fast rotation and translation structure was constructed by Qiu *et al.*[121] A 4.3 THz QWP with fast detection performance and a 4.2 THz QCL with CW operation mode have been used in the above system. The fast scanning reflection imaging of a hidden leaf has been demonstrated, with a single frame imaging time of less than 10 s and a maximum of 5000 points per second scanning speed. A resolution of 0.3 mm and a circular imaging region with a diameter of 100 mm were obtained.[121]

Due to the failure of Si readout integrated circuits (ROICs) and the thermal mismatch between the photo-detector arrays and the ROICs at temperatures below 40 K, there are big technical challenges to construct terahertz photo-type focal plane arrays. In 2016, a pixel-less photo-type terahertz imager based on the frequency up-conversion technique[122] was demonstrated by Fu *et al.*[123] The imager is composed of terahertz QWP and near-infrared (NIR) light emitting diodes (LEDs) which are called as QWP-LED and their materials are grown in sequence on the same substrates using MBE system. A laser spot of a 4.34-THz QCL was imaged by the QWP-LED together with a commercial Si camera. The imaging results show that the image blurring induced by the transverse spreading of photocurrent is negligible. The demonstrated pixel-less imaging opens a new way to realize high performance terahertz imaging devices. In addition, the terahertz QCLs also play an important role in scanning near-field optical microscope and a sub-micrometer resolution has been obtained.[124]

4. Conclusion and perspectives

In this paper, the working principle and the latest development of terahertz QCLs and QWPs are reviewed. The theoretical design for the active regions, waveguides, the performance optimization of devices, and the applications in terahertz photoelectric characterization technology and imaging are mainly presented. With regards to the terahertz QCL, as an important practical light source in terahertz range, it also needs to be further improved in the following aspects. Firstly, at present, without considering the power consumption of the refrigerator itself, the energy conversion efficiency of terahertz QCL is only less than 2%. The cooling of the laser is still a part that must be considered comprehensively in the system applications before the room-temperature operating of terahertz QCL is achieved. High operating temperature (greater than 77 K) and high energy conversion efficiency (greater than 2%) are needed for practical applications. Therefore, a more effective electric cooling method needs to be explored in addition to improving the energy conversion efficiency of the laser. Secondly, the improvement of the external coupling of the laser beam also needs further improvement, including the stability and reliability of the setups. Finally, in order to achieve multi-frequency imaging, the tunability of single mode operation of the laser is necessarily to be optimized. About the terahertz QWPs, in addition to improving the detection sensitivity, the up-conversion technology is an effective way to realize line array and array detection. Meanwhile, the integrations of ter-

ahertz laser source and detection device based on built-in amplifier, external waveguide, polarization converter, and other functional devices are also worth further investigation. It can be anticipated that the two devices, with constantly optimizing the performances, will play important roles in the applications of scanning near-field optical microscopy, ultrafast scanning tunneling microscopy with atomic-level resolution, biomedical imaging, biomedical effects research, etc.

Acknowledgment

The authors would like to thank professor Zhang-Hua Han for helpful discussion and suggestions, and careful reading of this manuscript.

References

[1] Köhler R, Tredicucci A, Beltram F, Beere H E, Linfield E H, Davies A G, Ritchie D A, Iotti R C and Rossi F 2002 *Nature* **417** 156
[2] Liu H C, Song C Y, SpringThorpe A J and Cao J C 2004 *Appl. Phys. Lett.* **84** 4068
[3] Tonouchi M 2007 *Nat. Photon.* **1** 97
[4] Liang G Z, Liu T and Wang Q J 2017 *IEEE J. Sel. Top. Quant.* **23** 1200118
[5] Mittleman D M 2018 *Opt. Express* **26** 9417
[6] Sizov F 2018 *Semicond. Sci. Technol.* **33** 123001
[7] Tan Z Y, Wan W J, Li H and Cao J C 2017 *Chin. Opt.* **10** 68 (in Chinese)
[8] Tan Z Y and Cao J C 2019 *Chin. J. Lasers* **46** 0614004 (in Chinese)
[9] Bosco L, Franckié M, Scalari G, Beck M, Wacker A and Faist J 2019 *Appl. Phys. Lett.* **115** 010601
[10] Wan W J, Li H and Cao J C 2018 *Opt. Express* **26** 980
[11] Li L H, Chen L, Freeman J R, Salih M, Dean P, Davies A G and Linfield E H 2017 *Electron. Lett.* **53** 799
[12] Wienold M, Röben B, Schrottke L, Sharma R, Tahraoui A, Biermann K and Grahn H T 2014 *Opt. Express* **22** 3334
[13] Wang X M, Shen C L, Jiang T, Zhan Z Q, Deng Q H, Li W H, Wu W D, Yang N, Chu W D and Duan S Q 2016 *AIP Adv.* **6** 075210
[14] Vitiello M S, Consolino L, Bartalini S, Taschin A, Tredicucci A, Inguscio M and De Natale P 2012 *Nat. Photon.* **6** 525
[15] Li H, Wan W J, Tan Z Y, Fu Z L, Wang H X, Zhou T, Li Z P, Wang C, Guo X G and Cao J C 2017 *Sci. Rep.* **7** 3452
[16] Zhou Z T, Zhou T, Zhang S Q, Shi Z F, Chen Y, Wan W J, Li X X, Chen X Z, Corder S N G, Fu Z L, Chen L, Mao Y, Cao J C, Omenetto F G, Liu M K, Li H and Tao T H 2018 *Adv. Sci.* **5** 1700982
[17] Kliebisch O, Heinecke D C, Barbieri S, Santarelli G, Li H, Sirtori C and Dekorsy T 2018 *Optica* **5** 1431
[18] Richter H, Greiner-Bär M, Pavlov S G, Semenov A D, Wienold M, Schrottke L, Giehler M, Hey R, Grahn H T and Hübers H W 2010 *Opt. Express* **18** 10177
[19] Kumar S 2011 *IEEE J. Sel. Top. Quant.* **17** 38
[20] Li L H, Chen L, Zhu J, Freeman J, Dean P, Valavanis A, Davies A G and Linfield E H 2014 *Electron. Lett.* **50** 309
[21] Kumar S, Hu Q and Reno J L 2009 *Appl. Phys. Lett.* **94** 131105
[22] Williams B S, Callebaut H, Kumar S and Hu Q 2003 *Appl. Phys. Lett.* **82** 1015
[23] Scalari G, Hoyler N and Faist J 2005 *Appl. Phys. Lett.* **86** 181101
[24] Liu H C, Wächter M, Ban D, Wasilewski Z R, Buchanan M, Aers G C, Cao J C, Feng S L, Williams B S and Hu Q 2005 *Appl. Phys. Lett.* **87** 141102
[25] Kumar S, Williams B S, Hu Q and Reno J L 2006 *Appl. Phys. Lett.* **88** 121123
[26] Worrall C, Alton J, Houghton M, Barbieri S, Beere H E, Ritchie D and Sirtori C 2006 *Opt. Express* **14** 171
[27] Lü J T and Cao J C 2006 *Appl. Phys. Lett.* **88** 061119
[28] Li H, Cao J C, Tan Z Y and Feng S L 2008 *J. Appl. Phys.* **104** 103101
[29] Freeman J R, Marshall O P, Beere H E and Ritchie D A 2008 *Opt. Express* **16** 19830
[30] Scalari G, Walther C and Faist J 2006 *Appl. Phys. Lett.* **88** 141102
[31] Kumar S, Chan CWI, Hu Q and Reno J L 2009 *Appl. Phys. Lett.* **95** 141110
[32] Wade A, Fedorov G, Smirnov D, Kumar S, Williams B S, Hu Q and Reno J L 2009 *Nat. Photon.* **3** 41
[33] Kumar S and Hu Q 2009 *Phys. Rev. B* **80** 245316
[34] Freeman J R, Madéo J, Brewer A, Dhillon S, Marshall O P, Jukam N, Oustinov D, Tignon J, Beere H E and Ritchie D A 2010 *Appl. Phys. Lett.* **96** 051120
[35] Kumar S, Chan C W I, Hu Q and Reno J L 2010 *Nat. Phys.* **7** 166
[36] Williams B S, Kumar S, Hu Q and Reno J L 2006 *Electron. Lett.* **42** 89
[37] Brandstetter M, Deutsch C, Krall M, Detz H, MacFarland D C, Zederbauer T, Andrews A M, Schrenk W, Strasser G and Unterrainer K 2013 *Appl. Phys. Lett.* **103** 171113
[38] Li L H, Zhu J X, Chen L, Davies A G and Linfield E H 2015 *Opt. Express* **23** 2720
[39] Ajili L, Scalari G and Faist J 2005 *Appl. Phys. Lett.* **87** 141107
[40] Fischer M, Scalari G, Walther C and Faist J 2009 *J. Cryst. Growth* **311** 1939
[41] Deutsch C, Krall M, Brandstetter M, Detz H, Andrews A M, Klang P, Schrenk W, Strasser G and Unterrainer K 2012 *Appl. Phys. Lett.* **101** 211117
[42] Deutsch C, Kainz M A, Krall M, Brandstetter M, Bachmann D, Schönhuber S, Detz H Zederbauer T, MacFarland D, Andrews A M, Schrenk W, Beck M Ohtani K Faist J Strasser G and Unterrainer K 2017 *ACS Photonics* **4** 957
[43] Vukmirovića N, Jovanović V D, Indjin D, Ikonić Z and Harrison P 2005 *J. Appl. Phys.* **97** 103106
[44] Bellotti E, Driscoll K, Moustakas T D and Paiella R 2008 *Appl. Phys. Lett.* **92** 101112
[45] Terashima W and Hirayama H 2015 *Proc. SPIE* **9483** 948304
[46] Popadic M, Milanovic V and Indjin D 2006 *J. Appl. Phys.* **100** 073709
[47] Bellotti E, Driscoll K, Moustakas T D and Paiella R 2009 *J. Appl. Phys.* **105** 113103
[48] Lynch S A, Bates R and Paul D J 2002 *Appl. Phys. Lett.* **81** 1543
[49] Lever L, Valavanis A, Ikonić Z and Kelsall R W 2008 *Appl. Phys. Lett.* **92** 021124
[50] Borak A 2005 *Science* **308** 638
[51] Luo H, Laframboise S R, Wasilewski Z R, Aers G C, Liu H C and Cao J C 2007 *Appl. Phys. Lett.* **90** 041112
[52] Kumar S, Williams B S, Qin Q, Lee A W M, Hu Q and Reno J L 2007 *Opt. Express* **15** 113
[53] Williams B S, Kumar S, Hu Q and Reno J L 2005 *Opt. Express* **13** 3331
[54] Fasching G, Benz A, Unterrainer K R 2005 *Appl. Phys. Lett.* **87** 211112
[55] Cao J C 2012 *Sci. China Inform. Sci.* **55** 16
[56] Cao J C, Li H, Han Y J, Tan Z Y, Lü J T, Luo H, Laframboise S and Liu H C 2008 *Chin. Phys. Lett.* **25** 953
[57] Zhang H, Dunbar L A, Scalari G, Houdré R and Faist J 2007 *Opt. Express* **15** 16818
[58] Benz A, Fasching G, Deutsch C, Andrews A M, Unterrainer K, Klang P, Schrenk W and Strasser G 2007 *Opt. Express* **15** 12418
[59] Amanti M I, Scalari G, Castellano F, Beck M and Faist J 2010 *Opt. Express* **18** 6390
[60] Mahler L, Tredicucci A, Beltram F, Walther C, Faist J, Beere H E and Ritchie D A 2010 *Appl. Phys. Lett.* **96** 191109
[61] Yu N, Wang Q, Kats M A, Fan J A, Khanna S P, Li L H, Davies A G, Linfield E H and Capasso F 2010 *Nat. Mater.* **9** 730
[62] Xu G, Colombelli R, Khanna S P, Belarouci A, Letartre X, Li L H, Linfield E H, Davies A G, Beere H E and Ritchie D A 2012 *Nat. Commun.* **3** 952
[63] Xu G, Li L, Isac N, Halioua Y, Davies A G, Linfield E H and Colombelli R 2014 *Appl. Phys. Lett.* **104** 091112
[64] Jin Y, Gao L, Chen J, Wu C Z, Reno J L and Kumar S 2018 *Nat. Commun.* **9** 1407
[65] Amanti M I, Fischer M, Scalari G, Beck M and Faist J 2009 *Nat. Photon.* **3** 586
[66] Wu C, Khanal S, Reno J L and Kumar S 2016 *Optica* **3** 734
[67] Biasco S, Garrasi K, Castellano F, Li L H, Beere H E, Ritchie D A, Linfield E H, Davies A G and Vitiello M S 2018 *Nat. Commun.* **9** 1122
[68] Mujagić E, Deutsch C, Detz H, Klang P, Nobile M, Andrews A M, Schrenk W, Unterrainer K and Strasser G 2009 *Appl. Phys. Lett.* **95** 011120

[69] Chassagneux Y, Colombelli R, Maineult W, Barbieri S, Beere H E, Ritchie D A, Khanna S P, Linfield E H and Davies A G 2009 *Nature* **457** 174

[70] Sevin G, Fowler D, Xu G, Julien F H, Colombelli R, Khanna S P, Linfield E H and Davies A G 2010 *Appl. Phys. Lett.* **97** 131101

[71] Liang G, Liang H, Zhang Y, Li L H, Davies A G, Linfield E H, Yu S F, Liu H C and Wang Q J 2013 *Opt. Express* **21** 31872

[72] Vitiello M S, Nobile M, Ronzani A, Tredicucci A, Castellano F, Talora V, Li L H, Linfield E H and Davies A G 2014 *Nat. Commun.* **5** 5884

[73] Biasco S, Beere H E, Ritchie D A, Li L H, Davies A G, Linfield E H and Vitiello M S 2019 *Light-Sci. Appl.* **8** 43

[74] Xu L, Curwen C A, Hon P W C, Chen Q S, Itoh T and Williams B S 2015 *Appl. Phys. Lett.* **107** 221105

[75] Curwen C A, Reno J L and Williams B S 2018 *Appl. Phys. Lett.* **113** 011104

[76] Xu L, Chen D, Curwen C A, Memarian M, Reno J L, Itoh T and Williams B S 2017 *Optica* **4** 468

[77] Curwen C A, Reno J L and Williams B S 2019 *Nat. Photon.* **13** 855

[78] Schneider H and Liu H C 2006 *Quantum well infrared photodetectors: Physics and applications*, (Berlin: Springer), pp. 45–80

[79] Guo X G, Tan Z Y, Cao J C and Liu H C 2009 *Appl. Phys. Lett.* **94** 201101

[80] Tan Z Y, Guo X G, Cao J C, Li H, Wang X, Feng S L, Wasilewski Z R and Liu H C 2009 *Semicond. Sci. Technol.* **24** 115014

[81] Guo X G, Cao J C, Zhang R, Tan Z Y and Liu H C 2013 *IEEE J. Sel. Top. Quant.* **19** 8500508

[82] Jia J Y, Wang T M, Zhang Y H, Shen W Z and Schneider H 2015 *IEEE Trans. Terahertz Sci. Technol.* **5** 715

[83] Luo H, Liu H C, Song C and Wasilewski Z R 2005 *Appl. Phys. Lett.* **86** 231103

[84] Franke C, Walther M, Helm M, Schneider H 2015 *Infrared Phys. Technol.* **70** 30

[85] Zhang R, Shao D X, Fu Z L, Wang H X, Zhou T, Tan Z Y and Cao J C 2017 *IEEE J. Sel. Top. Quant.* **23** 3800407

[86] Grant P D, Laframboise S R, Dudek R, Graf M, Bezinger A and Liu H C 2009 *Electron. Lett.* **45** 952

[87] Fathololoumi S, Dupont E, Ban D, Graf M, Laframboise S R, Wasilewski Z R and Liu H C 2010 *IEEE J. Quantum Electron.* **46** 396

[88] Tan Z Y, Zhou T, Cao J C and Liu H C 2013 *IEEE Photon. Technol. Lett.* **25** 1344

[89] Gu L, Tan Z Y, Wu Q Z, Wang C and Cao J C 2015 *Chin. Opt. Lett.* **13** 081402

[90] Gu L L, Zhang R, Tan Z Y, Wan W J, Yin R, Guo X G and Cao J C 2014 *J. Phys. D: Appl. Phys.* **47** 165101

[91] Zhang R, Fu Z L, Gu L L, Guo X G and Cao J C 2014 *Appl. Phys. Lett.* **105** 231123

[92] Palaferri D, Todorov Y, Chen Y N, Madeo J, Vasanelli A, Li L H, Davies A G, Linfield E H and Sirtori C 2014 *Appl. Phys. Lett.* **106** 161102

[93] Wang H X, Zhang R, Wang F, Jiao Z J, Shao D X, Fu Z L, Zhou T, Tan Z Y and Cao J C 2017 *Electron. Lett.* **53** 1129

[94] Wang H X, Fu Z L, Shao D X, Zhang Z Z, Wang C, Tan Z Y, Guo X G and Cao J C 2018 *Appl. Phys. Lett.* **113** 171107

[95] Zheng Y, Chen P, Yang H, Ding J, Zhou Y, Tang Z, Zhou X, Li Z, Li N, Chen X and Lu W 2019 *Appl. Phys. Lett.* **114** 091105

[96] Yang H, Zheng Y, Li N, Wang J and Chen P 2020 *J. Appl. Phys.* **127** 053104

[97] Tan Z Y, Guo X G, Cao J C Li H and Han Y J 2010 *Acta Physic. Sin.* **59** 2391 (in Chinese)

[98] Tan Z Y, Cao J C, Han Y J and Chen Z (U. S. Pantent) 8 749 225 B2 [20140610]

[99] Tan Z Y, Cao J C, Gu L and Zhu Y H (U. S. Pantent) 10 119 860 B2 [2018-11-06]

[100] Chen Z, Tan Z Y, Han Y J, Zhang R, Guo X G, Li H, Cao J C and Liu H C 2011 *Electron. Lett.* **47** 1002

[101] Chen Z, Gu L, Tan Z Y, Wang C and Cao J C 2013 *Chin. Opt. Lett.* **11** 112001

[102] Tan Z Y, Li H, Wan W J, Fu Z L, Wang C and Cao J C 2017 *Electron. Lett.* **53** 91

[103] Wan W J, Li H, Zhou T and Cao J C 2017 *Sci. Rep.* **7** 44109

[104] Li Z P, Wan W J, Zhou K, Liao X Y, Yang S J, Fu Z L, Cao J C and Hua Li H 2019 *Phys. Rev. Appl.* **12** 044068

[105] Li H, Li Z P, Wan W J, Zhou K, Liao X Y, Yang S J, Wang C J, Cao J C and Zeng H P 2020 *ACS Photonics* **7** 49

[106] Chan W L, Diebel J and Mittleman D M 2007 *Rep. Prog. Phys.* **70** 1325

[107] Hu B B and Nuss M C 1995 *Opt. Lett.* **20** 1716

[108] Darmo J, Tamosiunas V, Fasching G, Kröll J, Unterrainer K, Beck M, Giovannini M, Faist J, Kremser C and Debbage P 2004 *Opt. Express* **12** 1879

[109] Kim S M, Hatami F and Harris J S 2006 *Appl. Phys. Lett.* **88** 153903

[110] Li Q, Hu J Q and Yang Y F 2014 *Opt. Precision Eng.* **22** 2188 (in Chinese)

[111] Rothbart N, Richter H, Wienold M, Lutz Schrottke L, Grahn H T and Hübers H W 2013 *IEEE Trans. THz Sci. Technol.* **3** 617

[112] Lee A W M and Hu Q 2005 *Opt. Lett.* **30** 2563

[113] Lee A W M, Williams B S, Kumar S, Hu Q and Reno J L 2006 *IEEE Photon. Technol. Lett.* **18** 1415

[114] Oda N, Yoneyama H and Sasaki T 2008 *Proc. SPIE* **6940** 69402Y

[115] Oda N, Ishi T, Morimoto T, Sudou T, Tabata H, Kawabe S, Fukuda K, Lee A W M and Hu Q 2012 *Proc. SPIE* **8496** 84960Q

[116] Lee A W M, Qin Q, Kumar S, Williams B S and Hu Q 2006 *Appl. Phys. Lett.* **89** 141125

[117] Tan Z Y, Gu L, Xu T H, Zhou T and Cao J C 2014 *Chin. Opt. Lett.* **12** 070401

[118] Yang M W, Ji H B, Tan Z Y, Zhang H F, Wang Q, Peng N S, Gu J Q, Zhu Y M and Cao J C 2016 *Acta Optic. Sin.* **36** 0611004 (in Chinese)

[119] Zhou T, Zhang R, Guo X G, Tan Z Y, Chen Z, Cao J C and Liu H C 2012 *IEEE Photon. Technol. Lett.* **24** 1109

[120] Tan Z Y, Zhou T, Fu Z L and Cao J C 2014 *Electron. Lett.* **50** 389

[121] Qiu F C, Tan Z Y, Fu Z L, Wan W J, Li M Q, Wang C and Cao J C 2018 *Opt. Commun.* **427** 170

[122] Schneider H and Liu H C 2006 *Quantum well infrared photodetectors: Physics and applications*, (Berlin: Springer), pp. 161–164

[123] Fu Z L, Gu L L, Guo X G, Tan Z Y, Wan W J, Zhou T, Shao D X, Zhang R and Cao J 2016 *Sci. Rep.* **6** 25383

[124] Degl'Innocenti R, Wallis R, Wei B, Xiao L, Kindness S J, Mitrofanov O, Braeuninger-Weimer P, Hofmann S, Beere H E and Ritchie D A 2017 *ACS Photonics* **4** 2150